Quantum Chemical Evidence for an Intramolecular Charge-Transfer State in the Carotenoid Peridinin of Peridinin−Chlorophyll−Protein

Harsha M. Vaswani,[†,§] Chao-Ping Hsu,[#] Martin Head-Gordon,[†,‡] and Graham R. Fleming*[,†,§]

Department of Chemistry, University of California, Berkeley, Physical Biosciences Division and Chemical Sciences Division, Lawrence Berkeley National Laboratory, Berkeley, California 94720, and Institute of Chemistry, Academia Sinica, Nankang, Taipei, Taiwan 115

Received: January 23, 2003; In Final Form: May 2, 2003

We present theoretical confirmation of an intramolecular charge-transfer (CT) state in peridinin in agreement with experimental results of Frank and co-workers (*J. Phys. Chem. B* **1999**, *103*, 8751 and *J. Phys. Chem. B* **2000**, *104*, 4569). Quantum chemical calculations using time-dependent density functional theory under the Tamm−Dancoff approximation were made on two structures: fully optimized peridinin and a molecule from the crystal structure of peridinin−chlorophyll−protein. The CT state appears as the third and second excited singlet state, respectively, for the two structures. A dipole-in-a-sphere model is used to estimate the solvation stabilization energies of each state in a variety of solvents. The energy of the CT state is shown to decrease dramatically in solvents of increasing polarity while the energy of the dark S_1 (A_g^--like) state remains comparatively constant.

Introduction

Peridinin, found in peridinin−chlorophyll−protein (PCP), a light-harvesting complex from dinoflagellates, is an unusual carotenoid deserving special attention. The structure of PCP was determined by Hoffman et al.[1] and reveals that PCP is a trimer with each monomer containing eight peridinin (Per) and two chlorophyll (Chl) molecules divided quasi-symmetrically into two clusters. Peridinin is the only carotenoid known to have three full rings in its structure (see Scheme 1). In addition, it has an allene group, an epoxy group, and several carbonyl groups, including a lactone ring. These structural differences between peridinin and typical carotenoids could be related to the unusual function of peridinin in PCP. In assigning importance to the roles of carotenoids in light-harvesting complexes, the light-harvesting role is not generally vital, whereas their ability to provide photoprotection in the form of quenching of triplet chlorophylls, singlet oxygen, and perhaps singlet chlorophyll is necessary.[2−5] In PCP, however, the light-harvesting role of peridinin is essential for the organism's survival.[1]

The excited-state ordering of carotenoids such as peridinin, which deviate significantly from C_{2h} symmetry, is still a topic of intense interest. Within the C_{2h} symmetry group, the lowest excited singlet state has A_g^- symmetry, is optically dark, and is accessible via two-photon absorption from the ground state.[6,7] Strong absorption occurs to a state of approximate B_u^+ symmetry, generally called the S_2 state. The state is accessible from the ground state via one-photon, but usually not two-photon, spectroscopy. The B_u^+ state is primarily involved in the light-harvesting function of carotenoids.[8−13] A second optically dark state with B_u^- symmetry is predicted by multireference double excitation configuration interaction calculations using the Pariser−Parr−Pople Hamiltonian,[14] and may facilitate rapid internal conversion from the B_u^+ to the A_g^- state.[14−16] Experimental observation of this state[15−17] has proved controversial, and therefore we will retain the traditional convention of labeling A_g^- and B_u^+ as the first and second excited singlet states, respectively. To further complicate the matter, in some carotenoids, van Grondelle and co-workers have detected an additional excited-state called S* by means of femtosecond transient absorption spectroscopy.[18] The exact symmetry of the S* state has not yet been conclusively assigned. Finally, carotenoids with polar groups in their structure may have significantly different electronic structure than their nonpolar counterparts. In particular, they have the potential to form intramolecular charge-transfer (CT) excited states in addition to standard polyene levels. The spectral properties of the CT state form the focus of the present work via a computational study of the carotenoid peridinin.

SCHEME 1. Molecular Structure of Peridinin.

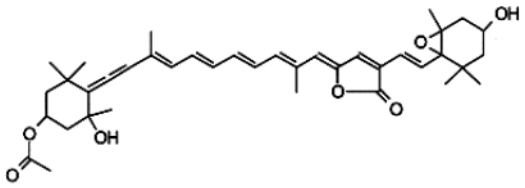

Strong evidence for the presence of an intramolecular CT state in peridinin has arisen from a variety of experiments. Time-resolved experimental studies of peridinin were the first to display peculiarities that could be the signature of a CT state. Akimoto et al. measured the S_1 fluorescence lifetime of peridinin in CS_2 to be 103 ps,[19] 10 times larger than the S_1 lifetime of β-carotene in *n*-hexane,[20,21] whereas the S_1 lifetime of peridinin in PCP was found to be under 3 ps. This suggests that the peridinin-to-chlorophyll energy transfer (Per → Chl) occurs predominantly via the S_1 state, even though the $S_0 \rightarrow S_1$ transition is not observed in the absorption spectrum. For nonpolar light-harvesting carotenoids, the dominant carotenoid-

* Corresponding author. E-mail: grfleming@lbl.gov.
† University of California, Berkeley.
§ Physical Biosciences Division, Lawrence Berkeley National Laboratory.
‡ Chemical Sciences Division, Lawrence Berkeley National Laboratory.
# Academia Sinica.

10.1021/jp030086t CCC: $25.00
Published on Web 07/04/2003

to-chlorophyll energy transfer is generally found to occur directly from the carotenoid S_2 state.[8−13]

The fluorescence results prompted solvent-dependent transient absorption studies of peridinin.[22] The S_1 lifetime was found to be strongly dependent on solvent polarity: 7 ps in trifluoroethanol and 172 ps in cyclohexane. The solvent-dependent transient absorption spectra of five other carotenoids were then obtained to investigate the molecular origin of this striking behavior.[23] For the carotenoids with carbonyl groups as part of their conjugated π-electron system (peridinin, fucoxanthin, and uriolide acetate), the excited singlet state lifetime depended strongly on the solvent polarity. Neoxanthin, a carotenoid that lacks a carbonyl group but is otherwise structurally very similar to peridinin, exhibits no solvent dependence in its transient absorption spectra. Frank et al. concluded that the presence of the carbonyl group as part of the conjugated π-electron system is the source of the solvent dependence.[23]

Time-resolved fluorescence spectra and visible to near-infrared transient absorption spectra of peridinin also displayed solvent dependence.[24] In nonpolar solvents, the fluorescence is attributed to the S_1 state. In polar solvents, the fluorescence intensity on the red edge of the emission spectrum is higher than in nonpolar solvents, and the vibronic structure observed in nonpolar solvents disappears. The fluorescence spectra observed in polar solvents consists of two overlapping bands, one of which was attributed to the S_1 state.[24] The near-infrared transient absorption of peridinin in methanol and in PCP reveals stimulated emission bands at 980 and 930 nm, respectively.[24,25]

Frank et al.,[23] Bautista et al.,[22] and Zigmantas et al.,[24] proposed a model, including the presence of an intramolecular CT state, to explain these dynamics. In this model, the CT state lies above S_1 (the Ag^--like state) in nonpolar solvents. In polar solvents, the CT state is stabilized more than the Ag^--like state and it becomes the lowest excited singlet state. The model can account for the drastic reduction of the Ag^--like state lifetime in polar solvents. The second band in the fluorescence spectra and the stimulated emission band observed in the near-infrared of the transient absorption spectra are both proposed to arise from the CT state.

Quantum chemical calculations of the electronic structure of peridinin have been carried out by several groups. Damjanovic et al. carried out semiempirical Pariser−Parr−Pople self-consistent field configuration interaction (PPP-SCF-CI) calculations and found that the carbonyl and methyl groups were important in mediating Per−Chl coupling.[26] More recently, Shima et al. used modified neglect of differently overlap using pseudospectral singles and doubles configuration interaction (MNDO−PSDCI) to investigate the electronic structure of peridinin in PCP.[27] These authors found significant CT character in the A_g^--like state, but no low-lying CT state distinct from the A_g^--like state. In contrast, Bautista et al. found a twisted intramolecular CT state arising from a HOMO (π chain) to LUMO (lactone ring) excitation. In the calculations of Bautista et al., only the conjugated π-electron portion of the carotenoid was used. The ground-state geometry of this structure was obtained by minimization using the AM1 Hamiltonian. The twisted structure consisted of a 90° rotation about the C−C single bond nearest the lactone ring toward the center of the compound. However, the crystal structure of PCP reveals that the peridinin molecules are twisted by, at most, 5° about the same C−C single bond.[1]

In view of the unusual electronic structure of peridinin and the lack of consensus on a model for the electronic states and the energy-transfer dynamics in PCP, we carried out ab initio electronic structure calculations via time-dependent density functional theory (TDDFT). Our goal was to determine whether a low-lying CT state could be found at the geometry adopted by peridinin in the PCP crystal structure, or in a fully optimized (vacuum) geometry unconstrained by the protein. We clearly observe a low-lying CT state in both geometries. To investigate the stabilizing influence of a polar environment, we also investigated a simple dielectric model for the transition energies of S_1 and S_{CT} in polar media.

Methods

The structures of peridinin 611 and 612 (nomenclature as per the Protein Data Bank file[28]) were obtained from the crystal structure of PCP.[1] Hydrogen atoms were added to the molecules using XPLOR[29] and classically minimized using the POWELL command in XPLOR. Semiempirical minimization of the hydrogen atoms was performed in MOPAC using the AM1 and PRECISE keywords. Ab initio optimization of hydrogen positions in peridinin 611 and all the coordinates of peridinin 612 were then performed in Q-Chem[30] using the Hartree−Fock method with the 3-21g* basis set, followed by the Becke3−Lee−Yang−Parr (B3LYP)[31] functional with the 6-31g* basis set.

Once optimized, TDDFT[32,33] and TDDFT with the Tamm−Dancoff approximation[34] (TDDFT/TDA) were used with the Slater−Vosko−Wilk−Nusair (SVWN)[35,36] functional and the 6-31++g* basis set to calculate properties of the first four singlet excited states. The technique has been used in earlier work to successfully characterize the electronic properties of linear conjugated polyenes and other carotenoids.[37,38] Unlike in configuration interaction singles (CIS)-type calculations, the dark S_1 state is characterized well by TDDFT/TDA.

The "plots" function in Q-Chem was utilized to visualize the molecular orbitals involved in transitions to the excited state. Excited states composed of a transition involving Kohn−Sham molecular orbitals with a different spatial localization were assigned to CT states. Such a CT character was subsequently confirmed by the attachment−detachment population analysis that shows a change in charge distribution regions. The other excited states, composed of transitions between π orbitals, were characterized as either A_g^--like or B_u^+-like states (or a mixture), according to symmetry rules depending on the approximate symmetry of the Kohn−Sham molecular orbitals involved in the transition.

A developmental version of Q-Chem was used in the present study. In addition to the excitation energies and oscillator strengths, we have also calculated the detachment and attachment densities.[39] The attachment and detachment density plots as well as the molecular orbitals displayed were produced using the output from the plot function in Q-Chem.

To estimate the dielectric solvation energy for each state, we calculated the difference density, defined as the difference between the attachment and detachment densities. The difference density yields the difference in electronic density of the excited and ground states. We calculated the expectation value of the dipole moment of the difference density. The permanent dipole moment of each excited state is obtained as the sum of the dipole moment calculated from the difference density and the ground-state dipole moment. A dipole-in-a-sphere model is used for estimating the solvation energy, ΔE (in eV),[40]

$$\Delta E = -\frac{0.529167*27.2107}{4.80298^2}\mu^2\frac{2}{a^3}\frac{\epsilon - 1}{2\epsilon + 1} \qquad (1)$$

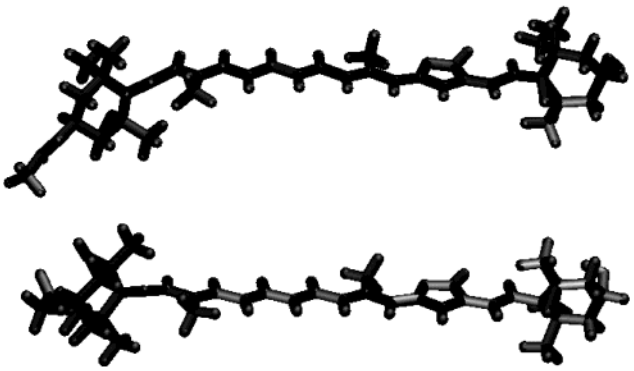

Figure 1. Geometry of peridinin 611 (top) and fully optimized peridinin (bottom).

TABLE 1: Excited States of Fully Optimized Peridinin from SVWN/6-31++g TDDFT/TDA and TDDFT Calculations**

states	E^a	λ^b	f^c	μ^d
		TDDFT/TDA		
$2A_g$-like	18 224	549	0.997	10.77
$1B_u$-like	19 461	514	1.8701	14.28
1CT-like	21 360	468	0.0801	2.82
$2B_u$-like	21 688	461	2.4922	15.62
		TDDFT		
state 1	16 837	594	2.6128	18.15
state 2	18 755	533	0.4582	7.20
state 3	20 795	481	0.3457	5.94
1CT	21 369	468	0.0055	0.73

[a] Excitation energies in wavenumbers. [b] Excitation wavelengths in nanometers. [c] Oscillator strengths. [d] Transition dipole moments in Debye.

where μ is the permanent dipole moment of the state in Debyes, a is the radius of the sphere in Å (assumed to be 12 Å), and ϵ is the dielectric constant of the solvent.

Results & Discussion

Excited Singlet States. Full optimization of peridinin using the B3LYP functional and the 6-31g* basis set give the structure of free Per shown in Figure 1. The results of our TDDFT and TDDFT/TDA calculations using the SVWN functional on free Per are presented in Table 1. Previous work showed that for polyene oligomers (butadiene to decapentaene) and the carotenoid rhodopin glucoside, the transition energy for the B_u^+-like state is typically underestimated by 0.4−0.7 eV using the SVWN, Becke−Lee−Yang−Parr (BLYP) or B3LYP exchange-correlation functionals in TDDFT calculations.[37,38] The underestimation of the B_u^+-like energy leads to unreliably high levels of mixing between the A_g^--like and B_u^+-like states. TDDFT/TDA calculations produce much more reasonable results.[37,38] As a result, we limit our discussion to the TDDFT/TDA calculations. It is clear from the results in Table 1 that peridinin is a unique carotenoid. In most carotenoids, the oscillator strength to the first excited state, the dark A_g^--like state, is very small. In free peridinin, we see substantial oscillator strength in this transition, most likely due to the proximity of S_2 to the S_1 state and the symmetry-breaking substituents. The two states are separated by only 1237 cm^{-1} with ∼25% of the S_1 population having B_u^+-like character (in the Kohn−Sham orbital representation this corresponds approximately to the HOMO → LUMO transition). The A_g^--like components still dominate the S_1 state with 25% of the population coming from a HOMO → LUMO+1 transition and 37% from a HOMO-1 → LUMO transition. Such high degrees of mixing is unusual in linear polyenes and most carotenoids, but expected in peridinin because of its substituents. However, the degree of mixing we calculate is too high: the calculated excited-state energy for the A_g^--like state is large, causing the energy gap between the A_g^--like and B_u^+-like states to be small. The error in the calculated excitation energy of the A_g^--like state is within the error of the TDDFT method. In contrast, the MNDO−PSDCI calculations of Shima et al.[27] place the A_g^--like state of all-trans peridinin at about 15 800 cm^{-1} and the B_u^+-like state at about 19 360 cm^{-1}. They calculate an oscillator strength of 0.23 for the A_g^--like state and 1.68 for the B_u^+-like state.

TABLE 2: Excited States of Peridinin 611 from SVWN/6-31++g TDDFT/TDA and TDDFT Calculations**

states	E^a	λ^b	f^c	μ^d
		TDDFT/TDA		
$2A_g$-like	16 394	610	0.0099	1.13
1CT-like	18 597	538	0.1007	3.39
$1B_u$-like	19 211	521	4.4382	22.15
2CT-like	21 138	473	0.0982	3.14
		TDDFT		
$1B_u$-like	15 642	639	3.4889	21.76
$2A_g$-like	16 320	613	0.046	2.44
1CT-like	18 600	538	0.006	0.82
state 4	20 908	478	0.1605	4.03

[a] Excitation energies in wavenumbers. [b] Excitation wavelengths in nanometers. [c] Oscillator strengths. [d] Transition dipole moments in Debye.

TDDFT/TDA results for Per 611 taken from the PCP structure are presented in Table 2. As can be seen in Figure 1, Per 611 (top) and free Per (bottom) have similar geometries except near the allene group. In Per 611, the allene group and its attached ring are twisted with respect to the conjugated backbone. The first excited state of peridinin in this conformation also corresponds to the A_g^--like state. In the fully optimized conformation, the proximity of S_2 to S_1 leads to significant mixing of the two states and significantly increases the oscillator strength to the A_g^--like state to 0.997. In Per 611, the first two excited states are further apart, and the oscillator strength to the A_g^--like state is 0.001, 2 orders of magnitude smaller than in free Per. Oscillator strengths of this transition in the different peridinin conformers found in PCP were also calculated using the MNDO−PSDCI method.[27] These calculations suggest much larger values of the oscillator strengths: between 0.32 and 1.09. A low oscillator strength of the transition to the A_g^--like state within the protein agrees with the experiment because no A_g^--like state is seen in the absorption spectrum of PCP. We calculate the S_1 state of Per 611 to be composed of two A_g components and no B_u components: 58% HOMO-1 → LUMO and 41% HOMO → LUMO+1. Our calculated gas-phase excitation energy for the A_g^--like state is 16 394 cm^{-1}, in reasonable agreement with the estimate of 17 340−23 790 cm^{-1} from MNDO−PSDCI calculations by Shima et al.[27] Figure 2 shows the difference between the nature of the transitions in free Per from those of Per 611. Attachment (green) and detachment (red) density plots are shown for the first four excited singlet states of free Per (left) and Per 611 (right). The transition from the ground state to S_1 is clearly mixed in free Per, whereas in Per 611 the same transition is an almost pure $\pi-\pi^*$ transition. The second excited state in free Per is mostly of B_u^+ character, with 24% A_g character, 45% a mixture of B_u and CT character, and 26% pure B_u character.

In Per 611, the second excited state is quite distinct from the A_g^- or B_u^+-like states described above and clearly shows substantial transfer of electron density from the epoxy and lactone rings to the polyene chain. We assign this state as the

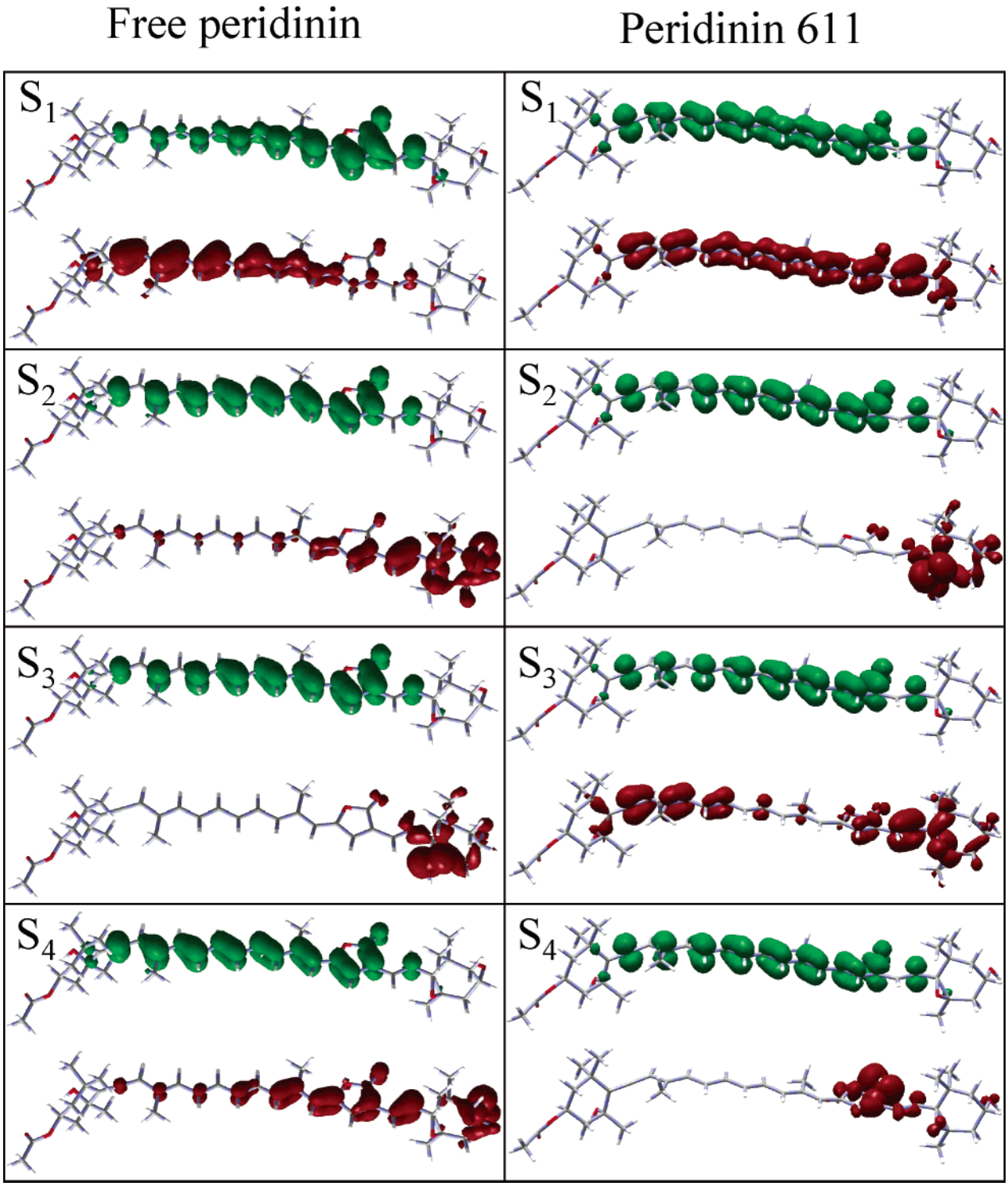

Figure 2. Attachment (shown in green) and detachment (red) density plots for fully optimized peridinin (left) and peridinin 611 (right). From top to bottom: S_1 attachment density, S_1 detachment density, S_2 attachment density, S_2 detachment density, S_3 attachment density, S_3 detachment density, S_4 attachment density, and S_4 detachment density.

CT state described in the Introduction. We calculated the transition dipole moment of the CT state to be 3.4 D. This value is very similar to the estimate of 3 D obtained from global analysis of ultrafast polarized transient absorption spectra conducted by Krueger et al.[41] MNDO−PSDCI calculations do not reveal a separate CT state.[27] Instead, substantial CT character is seen in the Ag^--like state.

For Per 611, the third excited state is purely B_u with contributions from two transitions: the HOMO → LUMO transition contributes 51% and HOMO-2 → LUMO contributes 37%. Unlike free Per, there is negligible mixing between the CT and the B_u^+-like states. We place the B_u^+-like state at 19 211 cm^{-1}, compared to the MNDO−PSDCI[27] estimate of ∼20 400 cm^{-1}.

The CT state appears as the third excited singlet state in free peridinin. The changes in electron density of the free Per CT and B_u^+-like states look similar to one another because of the large amount of mixing between the states. The CT state has a small oscillator strength of 0.080 and 0.100 in free Per and Per 611, respectively.

TABLE 3: Solvation Energy (ΔE) and Total Excitation Energy (E_{ex}) in Wavenumbers for Free Peridinin and Peridinin 611

state		water	CH_3CN	methanol	*n*-hexane
		Free Peridinin			
ground S	ΔE	−159	−155	−154	−60
$2A_g$-like	ΔE	−1955	−1912	−1903	−743
	E_{ex}	16 427	16 467	16 475	17 542
$1B_u$-like	ΔE	−7172	−7011	−6979	−2725
	E_{ex}	12 447	12 604	12 635	16 796
1CT-like	ΔE	−7453	−7286	−7253	−2832
	E_{ex}	14 065	14 229	14 261	18 589
$2B_u$-like	ΔE	−6256	−6116	−6088	−2377
	E_{ex}	15 591	15 728	15 754	19 372
		Peridinin 611			
ground S	ΔE	−152	−149	−148	−58
$2A_g$-like	ΔE	−815	−797	−794	−310
	E_{ex}	15 731	15 746	15 749	16 142
1CT-like	ΔE	−8377	−8189	−8152	−3183
	E_{ex}	10 372	10 556	10 593	15 472
$1B_u$-like	ΔE	−477	−467	−465	−181
	E_{ex}	18 885	18 893	18 894	19 088
2CT-like	ΔE	−4752	−4646	−4625	−1806
	E_{ex}	16 538	16 641	16 662	19 390

The appearance of a low-lying CT state in both geometries is consistent with the strong solvent dependence of the lifetime of the lowest excited state.[22,24] Frank and co-workers[23] attributed this effect to a CT state strongly coupled to the A_g^--like state: in nonpolar solvents the A_g^--like state is below the CT state, whereas in polar solvents the ordering of states is reversed. In the protein environment, these authors suggested that the CT state would be above the A_g^--like state. Of course, the energy of a state with significant CT character cannot be reliably obtained from vacuum calculation. Below we describe a simple dielectric calculation to estimate the solvent stabilization of this state.

The fourth excited state in free Per is mostly of B_u character and could be the elusive B_u^- state.[15−17] The S_4 state is composed of four components in its Kohn−Sham molecular orbital representation: 20% HOMO-3 → LUMO, 32% HOMO-2 → LUMO, 30% HOMO → LUMO, and 9% HOMO → LUMO+1. The first and last components listed have A_g character and comprise 29% of the state. The second component has both CT and B_u character, and the third component has B_u character.

In Per 611, we calculated the fourth excited state to be another CT state. Again, the electron density goes from being localized on the epoxy and carbonyl groups to be delocalized along the polyene chain. In addition, the oscillator strength of the transition is also small: 0.098.

Solvation Energies. Using eq 1 for the energy of a dipole-in-a-sphere and the ground- and excited-state dipole moments from the TDDFT/TDA calculations of free Per and Per 611, we calculated the total excitation energies and the solvation energies for both structures in four different solvents: water, methanol, acetonitrile, and *n*-hexane (Table 3). Although all of the states are stabilized more in polar than in nonpolar solvents, the stabilization energies for each state in a given solvent vary considerably. For example, in free peridinin, the CT state stabilization energy is 4621 cm^{-1} greater in water than in *n*-hexane, whereas the A_g^--like state is only stabilized by 1212 cm^{-1} in water with respect to *n*-hexane. The solvation energy is greater for the Per 611 CT state, where the CT state is stabilized by 5194 cm^{-1} in water compared to *n*-hexane, whereas the A_g^--like state is stabilized by only 505 cm^{-1} more in water than in *n*-hexane.

These simple calculations are in qualitative agreement with experimental results.[24] In the transient absorption experiments of peridinin in solution, a drastic decrease in lifetime of the A_g^--like state in polar solvents is observed. Zigmantas et al.[24] attribute this to a greater stabilization of the CT state in polar solvents. In nonpolar solvents, they speculate that the CT state lies above S_1, whereas in increasingly polar solvents, the energy of the CT state decreases compared to S_1 until it becomes the lowest excited singlet state. Our simple solvation model predicts the qualitative differences in solvent stabilization between the CT and the A_g^--like states. In free Per, we calculate the CT state to be above the A_g^--like state in *n*-hexane, but below the A_g^--like state in methanol.

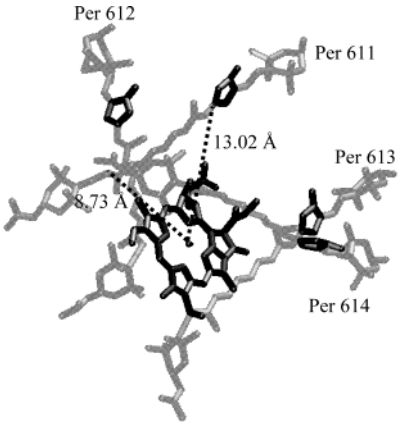

Figure 3. Geometry of peridinin (gray) and chlorophyll (black) in half a monomer of PCP. The lactone ring of peridinin is also shown in black.

Speculation on the Role of the CT State. In view of the dramatically different electron rearrangement involved in the A_g^--like and CT transitions, it is interesting to speculate on their relative Coulombic couplings to the Chl acceptor. Both states were calculated to lie above the Chl Q_y state, and, hence, can contribute to Per → Chl energy transfer. Figure 3 shows the arrangement of the peridinin and the Chl molecules in half of a monomer of PCP.[1] The Chl molecule lies with its center closer to the allene end of peridinin, away from the lactone ring. For example, in Per 611 the separation of the lactone ring from the Chl Mg atom is 13.02 Å, while the Mg−allene distance is 8.73 Å. The other Per molecules in PCP lie with the allene region even closer to the Chl, with separations ranging from 4.30 to 7.48 Å. The transition densities for the A_g^--like and CT transitions for Per 611 (Figure 4) show the expected characteristics: the A_g^--like state reveals extensive cancellation of positive and negative density along the entire molecule, while the CT transition involves mainly negative density at the lactone end and positive density at the allene end of the molecule. Although these results need to be confirmed by detailed numerical calculation, it seems likely that the Coulombic coupling between the Chl Q_y transition and the peridinin CT transition will be significantly larger than between the Chl Q_y and the S_0-S_1 transition. As a result, energy transfer will be enhanced from the CT state. Calculations based on the transition density cube method[42] for all peridinin conformers in PCP are currently underway.

Applicability of TDDFT to CT States. Finally, we comment on the applicability of TDDFT to CT states. Application of TDDFT to states with CT character is quite appropriate in principle, but can be problematic in practice because of limitations in the functionals currently available. As pointed out many years ago, DFT with local density approximation (LDA) would incorrectly dissociate NaCl into its constituent-charged species.[35] Such a ground-state CT problem can be solved by requiring the energy functional to have the correct derivative

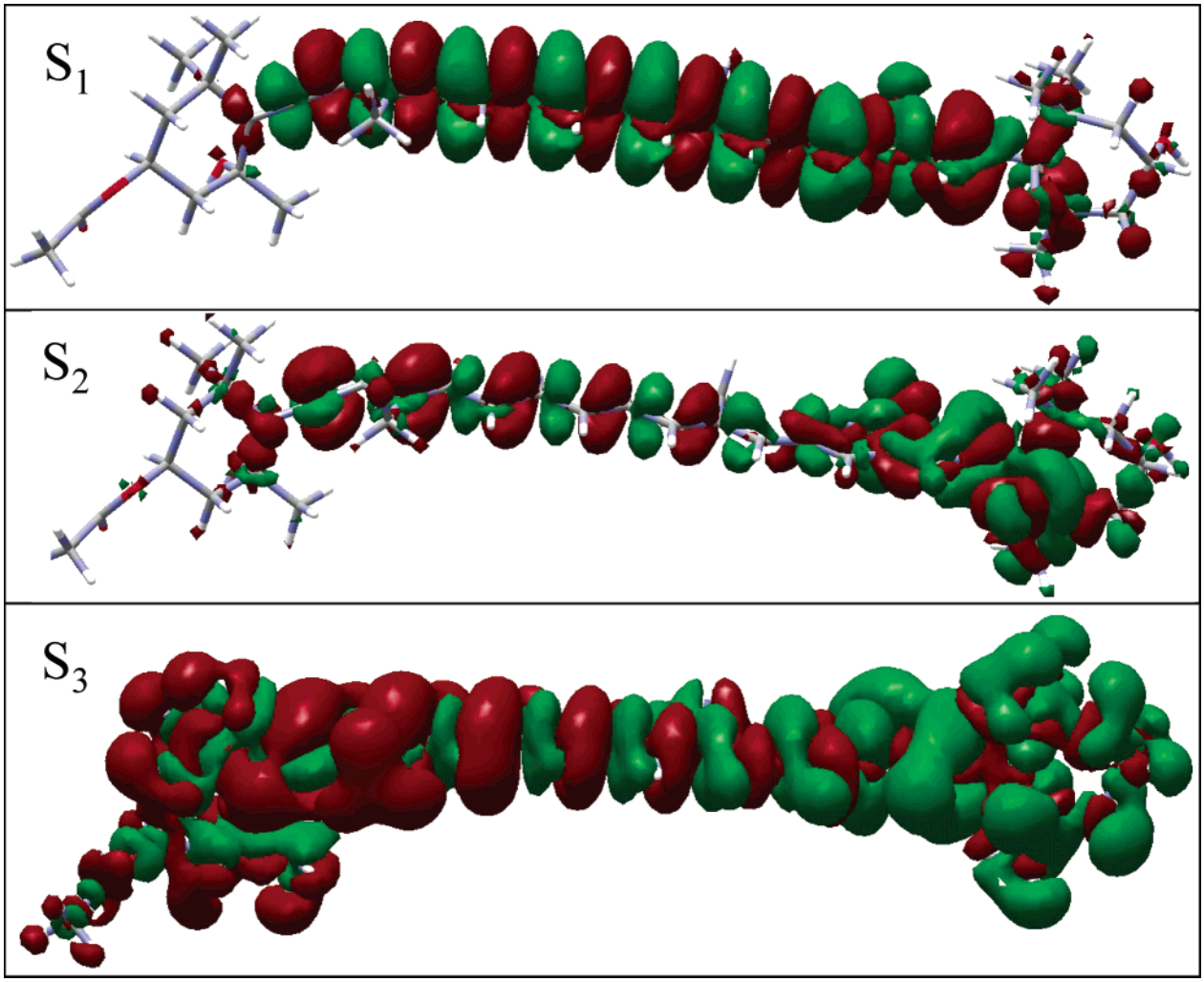

Figure 4. Excited-state transition densities of Per 611.

discontinuity with respect to electron density.[43] Likewise, a good description of CT properties of a molecule requires the proper derivative discontinuity in the energy functional. One simple, although somewhat ad-hoc way to incorporate the derivative discontinuity with an LDA functional, is the "shift and splice" approach.[44,45] In this method, the exchange-correlation potential in the core region is shifted by a constant value. Such a shift will play a role in correcting intermolecular CT problems, but may not be so critical in intramolecular CT systems such as that treated in the present study.

Recently there have been several studies using TDDFT (with conventional asymptotically incorrect functionals) for aromatic donor−acceptor systems with CT excited states. The results of Jamorski and co-workers,[46−48] for example, also support a twisted intramolecular charge transfer model for understanding the different fluorescence activities among the donor−acceptor systems studied. These calculations were performed using the B3LYP functional and the modified Perdew−Wang exchange and Perdew−Wang91 correlation functionals (MPW1PW91). The calculated excitation energies are generally within 0.2 eV of experimental estimates. TDDFT has also been used to successfully describe the electronic transitions of alkyl peroxy radicals,[49] a system where multiconfiguration self-consistent field calculations are not successful.[50] The phenyl peroxy radical absorption spectrum can be successfully described by TDDFT using the BLYP functional.[49] The visible band of this molecule results from a transition with a high percentage of double excitations and involves a significant transfer of electron density, both factors of importance in peridinin.

It is unclear which approximate functional is most appropriate to use to study vertical CT excited states, because all of the commonly used functionals do not have the right derivative discontinuity. The SVWN functional has been shown to give better results than B3LYP for the treatment of the dark S_1 (2^1Ag^-) state in polyenes.[37] The Coulombic coupling between the carotenoid Ag^--like dark state and the bacteriochlorophyll Q_y state has been obtained for a light-harvesting complex using the SVWN functional.[38] The coupling yielded carotenoid S_1 to bacteriochlorophyll Q_y excitation energy-transfer times that are in good agreement with experimental results. Our results seem to indicate that SVWN is a reasonable choice in characterizing the S_1 state in other carotenoids, including peridinin. We have also conducted test calculations of the fully optimized peridinin by using the BLYP functional and found that the differences between the SVWN and BLYP functional results are small (results not shown).

The recent success of TDDFT in calculating CT excited states and the success of the SVWN functional in characterizing carotenoids suggest that our method is appropriate for molecules such as peridinin. However, a final answer necessarily awaits further experimental or theoretical confirmation.

Summary

In this paper, we have presented quantum chemical evidence for a low-lying intramolecular CT state in peridinin using

TDDFT with the SVWN functional under the Tamm−Dancoff approximation. Our results suggest that, in vacuo, the CT state may lie above or below the B_u^+-like state, depending on the geometric structure of the molecule. The solvation energies of the excited states were calculated using a dipole-in-a-sphere model. In qualitative agreement with experimental results, the CT state of free peridinin is more strongly stabilized in polar solvents than the A_g^--like state. This results in the CT state falling below the A_g^--like state in polar solvents, while it remains above the A_g^--like state in nonpolar solvents. Similar calculations for the other native structures of peridinin in PCP, which all display a low-lying CT state, will be presented in a future work.

Acknowledgment. This work was supported by the Director, Office of Science, Office of Basic Energy Sciences, Chemical Sciences Division of the U.S. Department of Energy under contract number DE-AC03-76SF0098 and used resources provided by the National Energy Research Scientific Computing Center (contract number DE-AC03-76SF0098). C.P.H. acknowledges a start-up fund from Academia Sinica. We thank Nancy Holt for editing the manuscript.

References and Notes

(1) Hofmann, E.; Wrench, P. M.; Sharples, F. P.; Hiller, R. G.; Welte, W.; Diederichs, K. *Science* **1996**, *272*, 1788−1791.
(2) Renger, G.; Wolff, C. *Biochim. Biophys. Acta* **1977**, *460*, 47.
(3) Cogdell, R. J.; Frank, H. A. *Biochim. Biophys. Acta* **1987**, *895*, 63−79.
(4) Edge, R.; McGarvey, D. J.; Truscott, T. G. *J. Photochem. Photobiol., B* **1997**, *41*, 189−200.
(5) Ma, Y.-Z.; Holt, N. E.; Li, X.-P.; Niyogi, K. K.; Fleming, G. R. *Proc. Natl. Acad. Sci. U.S.A.* **2003**, *100*, 4377−4382.
(6) Walla, P. J.; Linden, P. A.; Hsu, C.-P.; Scholes, G. D.; Fleming, G. R. *Proc. Natl. Acad. Sci. U.S.A.* **2000**, *97*, 10808−10813.
(7) Walla, P. J.; Linden, P. A.; Ohta, K.; Fleming, G. R. *J. Phys. Chem. A* **2002**, *106*, 1909−1916.
(8) Krueger, B. P.; Scholes, G. D.; Jimenez, R.; Fleming, G. R. *J. Phys. Chem. B* **1998**, *102*, 2284−2292.
(9) Krueger, B. P.; Scholes, G. D.; Yu, J. Y.; Fleming, G. R. *Acta Phys. Pol., A* **1999**, *95*, 63−83.
(10) Damjanovic, A.; Ritz, T.; Schulten, K. *Phys. Rev. E* **1999**, *59*, 3293−3311.
(11) Andersson, P. O.; Cogdell, R. J.; Gillbro, T. *Chem. Phys.* **1996**, *210*, 195−217.
(12) Nagae, H.; Kakitani, T.; Katoh, T.; Mimuro, M. *J. Chem. Phys.* **1993**, *98*, 8012−8023.
(13) Scholes, G. D.; Harcourt, R. D.; Fleming, G. R. *J. Phys. Chem. B* **1997**, *101*, 7302−7312.
(14) Tavan, P.; Schulten, K. *J. Chem. Phys.* **1986**, *85*, 6602−6609.
(15) Sashima, T.; Nagae, H.; Kuki, M.; Koyama, Y. *Chem. Phys. Lett.* **1999**, *299*, 187−194.
(16) Sashima, T.; Koyama, Y. *J. Phys. Chem. B* **2000**, *104*, 5011−5019.
(17) Cerullo, G.; Polli, D.; Lanzani, G.; De Silvestri, S.; Hashimoto, H.; Cogdell, R. J. *Science* **2002**, *298*, 2395−2398.
(18) Papagiannakis, E.; Kennis, J. T. M.; van Stokkum, I. H. M.; Cogdell, R. J.; van Grondelle, R. *Proc. Natl. Acad. Sci. U.S.A.* **2002**, *99*, 6017−6022.
(19) Akimoto, S.; Takaishi, S.; Ogata, T.; Nishimura, Y.; Yamazaki, I.; Mimuro, M. *Chem. Phys. Lett.* **1996**, *260*, 147−152.
(20) Wasielewski, M. R.; Kispert, L. D. *Chem. Phys. Lett.* **1986**, *128*, 238−243.
(21) Frank, H. A.; Farhoosh, R.; Gebhard, R.; Lugtenburg, J.; Gosztola, D.; Wasielewski, M. R. *Chem. Phys. Lett.* **1993**, *207*, 88−92.
(22) Bautista, J. A.; Connors, R. E.; Raju, B. B.; Hiller, R. G.; Sharples, F. P.; Gosztola, D.; Wasielewski, M. R.; Frank, H. A. *J. Phys. Chem. B* **1999**, *103*, 8751−8758.
(23) Frank, H. A.; Bautista, J. A.; Josue, J.; Pendon, Z.; Hiller, R. G.; Sharples, F. P.; Gosztola, D.; Wasielewski, M. R. *J. Phys. Chem. B* **2000**, *104*, 4569−4577.
(24) Zigmantas, D.; Polivka, T.; Hiller, R. G.; Yartsev, A.; Sundstrom, V. *J. Phys. Chem. A* **2001**, *105*, 10296−10306.
(25) Zigmantas, D.; Hiller, R. G.; Sundstrom, V.; Polivka, T. *Proc. Natl. Acad. Sci. U.S.A.* **2002**, *99*, 16760−16765.
(26) Damjanovic, A.; Ritz, T.; Schulten, K. *Biophys. J.* **2000**, *79*, 1695−1705.
(27) Shima, S.; Ilagan, R. P.; Gillespie, N.; Sommer, B. J.; Hiller, R. G.; Sharples, F. P.; Frank, H. A.; Birge, R. R. *J. Phys. Chem.*, **2003**, *107*, ASAP on the Web May 6, 2003.
(28) Berman, H. M.; Westbrook, J.; Feng, Z.; Gilliland, G.; Bhat, T. N.; Weissig, H.; Shindyalov, I. N.; Bourne, P. E. *Nucleic Acids Res.* **2000**, *28*, 235−242.
(29) Brunger, A. T. *X-PLOR: A System for X-ray Crystallography and NMR*, version 3.1; Yale University Press: New Haven, CT, 1992.
(30) Kong, J.; White, C. A.; Krylov, A. I.; Sherrill, D.; Adamson, R. D.; Furlani, T. R.; Lee, M. S.; Lee, A. M.; Gwaltney, S. R.; Adams, T. R.; Ochsenfeld, C.; Gilbert, A. T. B.; Kedziora, G. S.; Rassolov, V. A.; Maurice, D. R.; Nair, N.; Shao, Y.; Besley, N. A.; Maslen, P. E.; Dombroski, J. P.; Daschel, H.; Zhang, W.; Korambath, P. P.; Baker, J.; Byrd, E. F. C.; Voorhis, T. V.; Oumi, M.; Hirata, S.; Hsu, C.-P.; Ishikawa, N.; Florian, J.; Warshel, A.; Johnson, B. G.; Gill, P. M. W.; Head-Gordon, M.; Pople, J. A. *J. Comput. Chem.* **2000**, *21*, 1532−1548.
(31) Becke, A. D. *J. Chem. Phys.* **1993**, *98*, 5648−5652.
(32) Casida, M. E. In *Recent Advances in Density Functional Methods*; Chong, D. P., Ed.; World Scientific Publishing: Singapore, 1995; Vol. 1, pp 155−192.
(33) Petersilka, M.; Gossmann, U. J.; Gross, E. K. U. *Phys. Rev. Lett.* **1996**, *76*, 1212−1215.
(34) Hirata, S.; Head-Gordon, M. *Chem. Phys. Lett.* **1999**, *314*, 291−299.
(35) Slater, J. C. *The Self-Consistent Field for Molecules and Solids I: Quantum Theory for Molecules and Solids*; McGraw-Hill: New York, 1974; Vol. 4.
(36) Vosko, S. H.; Wilk, L.; Nusair, M. *Can. J. Phys.* **1980**, *58*, 1200−1211.
(37) Hsu, C.-P.; Hirata, S.; Head-Gordon, M. *J. Phys. Chem. A* **2001**, *105*, 451−458.
(38) Hsu, C.-P.; Walla, P. J.; Head-Gordon, M.; Fleming, G. R. *J. Phys. Chem. B* **2001**, *105*, 11016−11025.
(39) Head-Gordon, M. *J. Phys. Chem.* **1995**, *99*, 14261−14270.
(40) Bottcher, C. J. F. *Theory of Electric Polarization*; Elsevier Science: New York, 1915.
(41) Krueger, B. P.; Lampoura, S. S.; van Stokkum, I. H. M.; Papagiannakis, E.; Salverda, J. M.; Gradinaru, C. C.; Rutkauskas, D.; Hiller, R. G.; van Grondelle, R. *Biophys. J.* **2001**, *80*, 2843−2855.
(42) Krueger, B. P.; Scholes, G. D.; Fleming, G. R. *J. Phys. Chem. B* **1998**, *102*, 5378−5386.
(43) Perdew, J. P.; Parr, R. G.; Levy, M.; Balduz, J. L. J. *Phys. Rev. Lett.* **1982**, *49*, 1691−1694.
(44) Casida, M. E.; Casida, K. C.; Salahub, D. R. *Int. J. Quantum Chem.* **1998**, *70*, 933−941.
(45) Casida, M. E.; Salahub, D. R. *J. Chem. Phys.* **2000**, *113*, 8918−8935.
(46) Jödicke, C. J.; Lüthi, H. P. *J. Chem. Phys.* **2002**, *117*, 4146−4156.
(47) Jödicke, C. J.; Lüthi, H. P. *J. Chem. Phys.* **2002**, *117*, 4157−4167.
(48) Jamorski, C.; Foresman, J. B.; Thilgen, C.; Lüthi, H.-P. *J. Chem. Phys.* **2002**, *116*, 8761−8771.
(49) Weisman, J. L.; Head-Gordon, M. *J. Am. Chem. Soc.* **2001**, *123*, 11686−11694.
(50) Krauss, M.; Osman, R. *J. Phys. Chem.* **1995**, *99*, 11387−11391.